Iranian Journal of Science and Technology, Transactions of Mechanical Engineering (2025) 49:181–200
https://doi.org/10.1007/s40997-025-00837-7

RESEARCH PAPER

Effect on Machinability Characteristics of Cryogenic Process and Performance Assessment by Using Machine Learning Approach with Scaled Conjugate Gradient Algorithm

Mehmet Akkaş[1] · **Mehmet Gürdal**[1]

Received: 12 September 2024 / Accepted: 10 January 2025 / Published online: 4 February 2025

Abstract

The present investigation is focused on the machinability and characterisation of cryogenised AISI 4140 steels, which are renowned for exhibiting superior hardness, durability, wear resistance, dimensional and chemical stability, and fatigue strength when compared to conventional steels. Hard turning experiments were conducted on cryogenised steel specimens employing dry cutting conditions with a carbide insert. As the cutting tip, the TT5100 quality TIN coated type with code WNMG 080408 MT produced by TaeguTec company was used. The study examines the impact of various cutting parameters, including three distinct cutting speeds (160, 200, 240 m/min), three feed rates (0.04, 0.08, 0.12 mm/rev), and three depths of cut (0.1, 0.15, 0.2 mm), on power consumption and surface roughness values. The utilisation of the artificial neural network (ANN) approach, a machine learning methodology, for the analysis of measured values adds another layer of originality to the research. Transfer functions, such as Scaled Conjugate Gradient (Trainscg), were employed within the ANN structure. The calculated metrics include a mean absolute error (MAE) of 0.0218, 0.0542, and 0.0064, and a mean squared error (MSE) of 0.0429. The mean absolute error (MAE) was 0.0683, the mean squared error (MSE) was 0.0429, and the mean relative deviation (ARD%) was 10.71%, 0.0718%, and 0.2020%. Furthermore, the optimal values for the correlation coefficient (R^2) were determined as 0.9512, 0.9999, and 0.9997.

Keywords AISI 4140 cryogenized · CBN tool · Hard turning · Surface roughness · Machinability · Characterization

Abbreviations

ANN	Artificial neural network
ARD	Average relative deviation (%)
b	Bias
EDS	Energy dispersive spectrum
I	Current (A)
L	Sound (dB)
Ldm	Learngdm (transfer function)
MAE	Mean absolute error
MSE	Mean square error
MLP	Multilayer perceptron
w	Weight
R^2	Correlation coefficient
Ra	Surface roughness
SEM	Scanning electron microscopy
SCG	Scaled conjugate gradient
Tsg	Tansig (transfer function)

✉ Mehmet Gürdal
mgurdal@kastamonu.edu.tr

[1] Department of Mechanical Engineering, Kastamonu University, Kastamonu, Turkey

1 Introduction

Hard turning has emerged as a viable approach for machining automotive components crafted from iron alloys with a hardness exceeding 45 HRC. This method offers a reduction in both delivery time and production cost, eliminating certain processing steps and procedures that are inherent to classical machining processes for hard iron alloy materials. For instance, a hard-turned gear shaft with a hardness of 59–62 HRC has been observed to reduce the cycle time by 80% (Rashid et al. 2001; Rashid 2014). Hardened steel materials are frequently employed in the production of essential components in the aviation and automotive industries due to their distinctive properties, including hardness, toughness, and weldability. For instance, hardened AISI 4140 steel is employed in the production of automotive components, including shafts, gears, and bearings. In hard turning, hardened steel materials are particularly susceptible to high temperatures due to the high friction between the tool and the workpiece. It is evident that elevated temperatures have a significant impact on the quality of the material (Sayuti et al. 2014). The global population is expanding, which is leading to an increase in energy consumption. The expansion of living standards, concomitant with population growth, has the effect of increasing the utilisation of machines. As machines become more prevalent in human life, so too does energy consumption increase. Consequently, as production levels rise, so too does the production of machines. The limited energy reserves available globally have made energy efficiency one of the most pressing issues. Concurrently, the necessity for energy results in elevated energy costs. The operation of the machines employed in the manufacturing industry is contingent upon the generation of electrical energy. The majority of electrical energy is derived from fossil fuels. The combustion of fossil fuels releases harmful gases into the atmosphere, which accumulate and create a greenhouse gas effect. The elevated temperature results in further evaporation. As the amount of evaporation increases, the greenhouse gas effect becomes more pronounced, leading to further evaporation. The increased temperature causes glaciers to melt, thereby increasing the water level. This, in turn, submerges settlements, which reduces the habitats and agricultural lands. The rise in temperature has been linked to global climate degradation, which in turn has been linked to the occurrence of storms in some regions and droughts in others. Both of these phenomena have been identified as posing a threat to human life. The damage to agricultural products caused by floods and storms, coupled with the increasing global population, will result in a further deterioration of global nutritional standards. Malnutrition will facilitate the spread of epidemics. Given the aforementioned circumstances, the issue of energy efficiency is becoming increasingly pertinent. In the field of energy efficiency, machine parts with higher yields, dependent on the time of use, are provided with machines with lower surface quality. Furthermore, machines with low surface roughness values reduce energy losses due to low friction forces. Upon examination of the studies on hard turning, it was found that the researchers had focused on the effect of tool geometry (Thiele and Melkote 1999; Özel et al. 2005) tool wear (Poulachon et al. 2001; Grzesik 2008), cutting temperature and cutting forces (Huang and Liang 2005). In their study, Das et al. (2015a) reported that the optimal surface quality was achieved at a feed rate of 0.05 mm/rev. The cutting speed was set at 170 m/min, with a depth of cut of 0.2 mm. On the other hand, Rashid et al. (Rashid et al. 2016) demonstrated that machining of AISI 4340 steel with a CBN cutting tool can result in a surface roughness of 45 nm without the need for additional tools. It was highlighted that the most significant factor influencing surface roughness in hard turning is the low feed rate (approximately 0.02 mm/rev), which accounts for 99.16% of the total effect. Furthermore, the study revealed that a reduction in the feed rate leads to enhanced surface finish while concurrently reducing the tool's lifespan. demonstrated that the optimal cutting parameters for achieving the lowest cutting temperature and lowest cutting force are a cutting speed of 615 m/min. The optimal feed rate was found to be 0.3 mm/rev, with a depth of cut of 0.5 mm. Furthermore, it has been established that the feed rate exerts the greatest influence on both the cutting temperature and cutting force. Das et al. (Das et al. 2015b) observed that an increase in cutting speed resulted in a decline in surface roughness. In a study published in 2015, Agrawal et al. evaluated surface roughness during the processing of AISI 4340 steel (69 HRC) and employed multiple regression models in their investigation. In a study conducted by Sharma (2019), the maximum value of surface roughness was achieved in hard turning in a dry environment with parameters of 100 mm/s cutting speed. The feed rate was set at 0.12 mm/rev, while the depth of cut was 0.3 mm. In the case of turning AISI 4340 steel, it has been demonstrated that solid lubricant conditions are the most favourable in comparison to wet and dry conditions across the entire range of process parameters. The results of the aforementioned studies indicate that the optimal cutting conditions for hard turning are a cutting speed of 300–600 m/min, a feed rate of 0.05–0.5 mm/rev, and a depth of cut of 0.2–1 mm (Das et al. 2015a, b; Agrawal et al. 2015; Rashid et al. 2016; Sharma 2019; Singh et al. 2019). The quality of the surface of a material affects its properties in a number of ways. These include friction, wear, lubrication, and coating. The effects of these properties determine the corrosion resistance, fatigue resistance, friction resistance, and service life of the material. For these reasons, surface quality has become a basic requirement for many applications (Asakura and Yan 2014). In order to fulfil this requirement, a number of different methods have been employed in the field of hard turning. Another one of these, Gaitonde et al. (2009) investigated the impact of depth of cut and machining time on machinability characteristics, including machining force, power, specific cutting force, surface roughness, and tool wear, during hard turning of high chromium AISI D2 cold work tool steel. With the advancement of technology, the range of materials utilized in industry is expanding continuously. However, in order to select the most appropriate, most accurate and most economical material from the plethora of options available, it is necessary to possess a comprehensive understanding of the material in question, encompassing its physical, chemical, and mechanical properties. In general, the most preferred material is the most efficient and economical material that provides the desired conditions in general. (Özlü et al. 2023). The most cost-effective, practical, and productive material for our work is AISI 4140 steel.

The presence of chromium and molybdenum in AISI 4140 steel results in the formation of a hard martensitic structure following heat treatment. The formation of this structure confers upon AISI 4140 steel a range of mechanical properties, including strength, toughness, wear resistance and ductility. These properties have been gained as a result of the aforementioned mechanical properties. AISI 4140 steel is a material of choice in the aviation and automotive industries (Choo et al. 2000; Kam 2020).

In the cryogenic process, materials are cooled to extremely low temperatures, thus enabling the desired metallurgical and microstructural properties to be achieved. This process is typically employed to enhance the abrasion resistance of materials with high abrasion. Once the process has been applied, it becomes a permanent feature of the material and affects the entire region (Jamali et al. 2019). In the cryogenic process, the material is typically maintained at the desired temperature and time. Subsequently, the material is heated to a temperature within a specified range. The process is conducted at subzero temperatures (in the range of − 125 and − 196 °C) and involves the conversion of the entire structure to martensite, the formation of fine carbide deposits and the homogenisation of the Fe–C distribution by cryogenic means. This heat treatment offers the potential to enhance the material's toughness without affecting its hardness (Kam and Saruhan 2021). Consequently, the mechanical properties of heat-treated materials undergo notable enhancements, including improvements in abrasion resistance, strength, and hardness. In the present era, the cryogenic process is a widely preferred method for enhancing the mechanical properties of materials. The cryogenic process is employed in a multitude of industries, including the aviation and automotive sectors (Kam 2020; Agrawal et al. 2024; Jadhav and Sahai 2024).

The initial step is to select the optimal cutting tool, contingent upon the selected material and intended use. In selecting a cutting tool, it is essential to consider the properties of the material in question and the desired level of machining accuracy. It is of great importance to select the most efficient, most economical, and most suitable cutting tool for the sustainability of experimental studies. Once the cutting tool and material have been selected, it is important to consider the cutting parameters. In determining the cutting parameters, it is essential to consider the type of cutting tool and the dimensions of the material. The determination of optimal cutting parameters serves to reduce vibration during machining and to minimise surface roughness and tool wear (Risbood et al. 2003; Das et al. 2015a; Swain et al. 2020; Özlü et al. 2023). Rashid et al. (2016) processed AISI 4340 steel without the use of additional tools, employing a CBN cutting tool to achieve a surface roughness of 45 nm. Grzesik et al. (2017) observed that the surface roughness of hard materials was significantly reduced when machining with CBN cutting tools. Besides, Żak (2017) observed that the device in question exhibited significantly lower roughness values on hard surfaces when utilising CBN cutting tools. Ginting et al. (2017) posited that a CBN cutting tool is essential for attaining both high dimensional precision and high surface quality. The findings of these literature studies indicate that… In this study, a CBN cutting tool was employed. The present study aimed to investigate the effects of various factors, including cutting parameters, vibration, and noise, on surface roughness and tool wear. To address this limitation, contemporary research has exhibited a proclivity towards employing artificial intelligence (AI)-based models, specifically those grounded in artificial neural networks (ANN) (Zain et al. 2010). Muthukrishnan and Davim (2009) propose the implementation of ANN-based models, citing their reduced computational time and heightened precision. In a study by Ozel and Karpat (2005), the application of artificial neural network (ANN) modelling techniques was found to enhance the prediction accuracy of surface roughness and tool flank wear in finish hard turning. The authors endorsed the segmentation of each response for optimal modelling. The utility of the ANN model, a machine learning methodology, extends to the estimation of machinability parameters. A variety of techniques are employed within the ANN model for the purpose of prediction, with the Feed Forward Neural Network (FFNN) method being a particularly prevalent example (Sazlı 2006). Akkuş and Asiltürk (Akkus 2011) devised an innovative model utilising fuzzy logic, artificial neural networks, and multi-regression to ascertain surface roughness values for AISI 4140 grade tempered steel. The

Fig. 1 Flowchart of experimental studies

Fig. 2 TTC 630 model CNC lathe belonging to Taksan company, **a** Sound **b** Surface roughness and **c** Current measuring device

evaluation, based on the Mean Squared Error (MSE), facilitated a comparative analysis of the three models. Karayel (2009) explored the surface roughness of AISI 1050 steel using a multilayer artificial neural network (ANN) with a feed-forward architecture. The ANN was trained and tested using experimental data, and the resulting ANN results demonstrated a significant correlation with empirically measured outcomes. Neseli et al. (2009) conducted a series of tests with varying approximation and cutting angles. The ANN training stage employed data derived from experiments to evaluate Average Ra values based on the nose radius, approximation angle, and rake angle. In addition, Gaitonde et al. (2011) employed ANN modelling to examine the influence of tool material, cutting speed, feed rate, and machining time on specific cutting force, surface roughness, and tool wear in hard turning. It is noteworthy that the approach taken is to model each response independently. Lin et al. (2001) employed abductive network models to predict cutting force and surface roughness, capitalising on the network's capacity to automatically identify an optimal architecture through the Predicted Square Error (PSE) criterion. The results demonstrated superior performance in comparison to multiple regression models. In a recent endeavor, Mia et al. (2017) employed artificial neural networks (ANNs) to predict surface roughness in hard turning of 600 BHN steel under the application of minimum quantity lubrication (MQL). The study achieved a precision level of 97.5%.

Previous studies have demonstrated the characterisation of semi- and medium-hardened states of AISI 4140 steel and their machinability capabilities. However, there has been a

Table 1 Chemical composition of AISI 4140 steel (Rooprai et al. 2022)

Elemets	Fe	C	Si	Mn	S	P	Cr	Mo
wt(%)	Bal	0.382	0.230	0.930	0.006	0.005	0.900	0.218

paucity of research on the machinability of cryogenised AISI 4140 steel. Furthermore, the fact that its characterisation has not yet been addressed is a significant motivation for this study. In light of these considerations, the characterisation analysis of cryogenised AISI 4140 steel, its machinability capabilities and a comparison of the results with machine learning serve to emphasise the original aspect of the study. Furthermore, the lack of sufficient research on hard turning of cryogenised AISI 4140 steels represents another important motivation for this study. The principal objective of this study is to examine and contrast the influence of diverse machining parameters on current, sound, and surface roughness, employing an artificial neural network approach.

2 Material and Method

In this study, it has been investigated experimental and machine learning approach for machinability characteristics such as current, sound, and surface roughness parameters by taking considered AISI 4140 cryogenized. In context, this section has been analyzed as two parts. Firstly, it was evaluated experimentally machinability variables. Afterwards, it has been compared prediction performances as using ANN method that machine learning method. General investigation phases of the study have been showed in Fig. 1. As understood as in Fig. 1, total evaluation processes is made of eight steps.

2.1 Experimental Approach

AISI 4140 material was used in experimental studies. Samples with a diameter of 50 mm and a length of 100 mm were prepared and subjected to turning under dry cutting conditions. The workpiece material was suddenly cooled in oil after standing at 950 ℃ for 2 h. By applying vacuum hardening technique, homogeneity is provided in heat treatment. To remove the tension of the material, tempering was done at 350 ℃. It is tested whether the desired features are gained or not. 53 HRC hardness value has been reached. The material is tied between the tailstock and the chuck. Some material was removed from the surface and prepared for machining experiments. With the developments in material and heat treatment technology, the issue of machinability is on the agenda. After obtaining high mechanical strength, machinability of the material is one of the most important

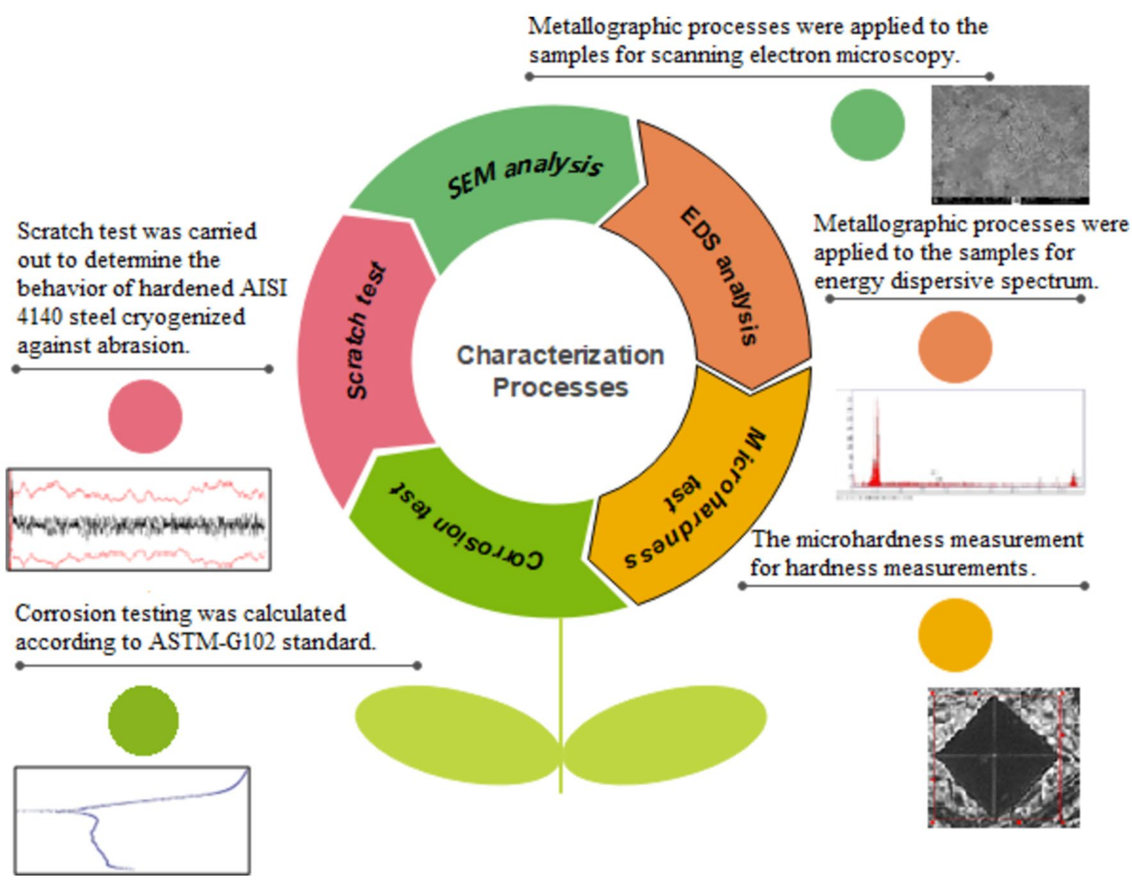

Fig. 3 Flowchart of characterization processes

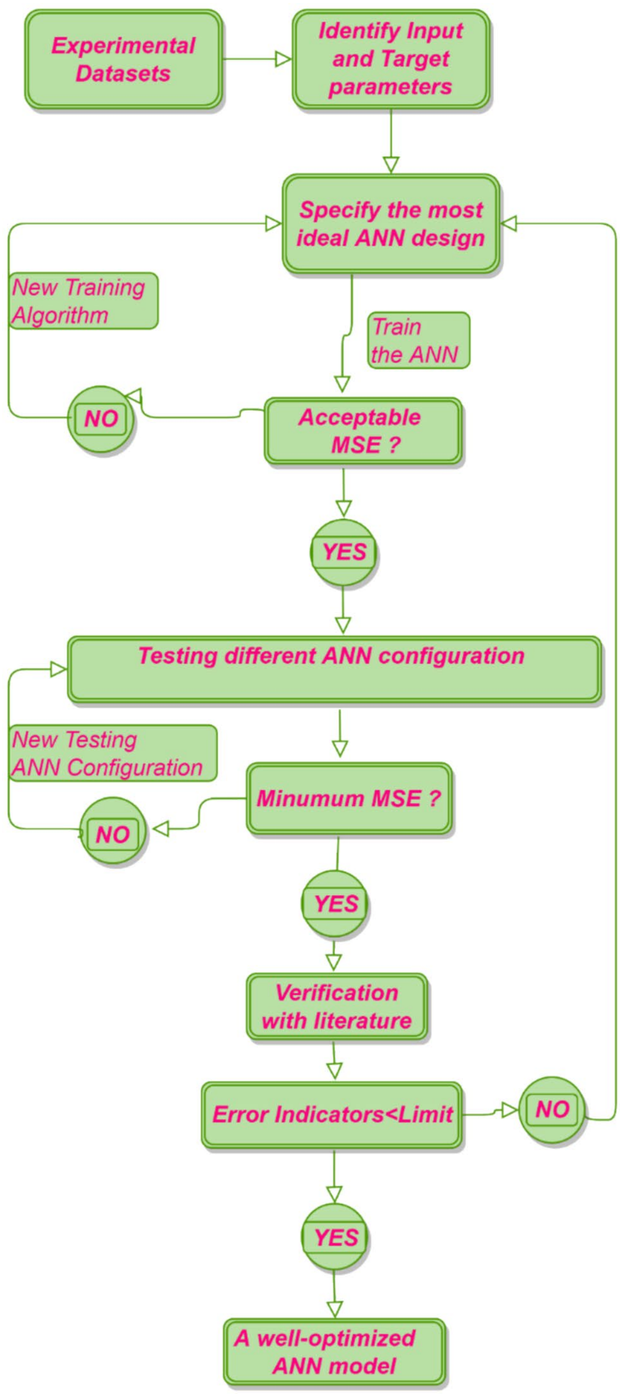

Fig. 4 Flow chart of machine learning model

problems. These materials need to be processed in high rigidity machine tools.

While determining the cutting parameters, the cutting values recommended for the cutting tool in existing literature studies were used. The turning process was carried out on a TTC 630 model CNC lathe belonging to Taksan company (Fig. 2). As the cutting edge, TT5100 quality TIN coated type with code WNMG 080408 MT, produced by TaeguTec company, was used. MWLNR 25 × 25 M08 model from MBC company was used as the tool holder. Sound intensity was measured with a Lutron SL-401 (Fig. 2a) sound intensity meter in Slow position, during the time when the ambient sound was lowest. The distance between the device and the mirror is 1 m. Pro Vibro brand PVM 303 model device (Fig. 2b) was used for vibration measurement. The magnetic probe of the device is attached to the mirror of the bench. The device measured in mm/s position. The current value passing through a phase was measured with a UNI-T UT201 clamp meter (Fig. 2c). The total current value was calculated by multiplying the current value by three. The surface roughness value was measured with a Mitutoyo SJ 201 roughness measuring device by selecting a sampling length of 0.8 mm. For each value, measurements were taken at three separate points and the average roughness value was calculated. In experimental studies, vibration, sound intensity, and current values were recorded instantly. After each experimental study, the workpiece was taken from the mirror and the surface roughness value was measured. The execution order of the processing experiments and the methods are shown in Fig. 1. On the other hand, the chemical composition of AISI 4140 steel examined in this study is given in Table 1.

The samples underwent metallographic preparation to enable analysis through energy dispersive spectroscopy (EDS) and scanning electron microscopy (SEM). The metallographic processes included sequential sanding, polishing, and etching. Sanding was performed using abrasives of 200, 360, 600, 1000, and 1200 mesh sizes in succession. Polishing was subsequently carried out with 3 µm and 1 µm diamond solutions to achieve a smooth surface finish. Following this, the samples were etched using a prepared etching reagent. SEM imaging was conducted using an "FEI QUANTA 250 FEG" instrument at Kastamonu University's Central Research Laboratories. Additionally, the microhardness of the samples was determined using a microhardness testing method. The microhardness measurements were conducted in the Mechanical Engineering Department Laboratory of Kastamonu University using a SHIMADZU HMV-G21 model microhardness tester, applying an HV 0.3 kg load. A force of 300 g was exerted for 16 s to evaluate the microhardness. Corrosion measurements were performed in the Mechanical Engineering Research Laboratory using the Reference 3000 Potentiostat/Galvanostat/ZRA instrument. Before corrosion testing, the prepared samples were ultrasonically cleaned sequentially in acetone, distilled water, and ethanol for 15 min at 35 °C. Subsequently, the samples were dried in an oven at 60 °C for 45 min. The corrosion rates were calculated based on data from the device, following the ASTM-G102 standard (2023). Before the abrasion test, the samples were sanded with 400, 600, 1000, and 1200 mesh sandpaper and their surfaces were polished with diamond

Fig. 5 **a** Basic topology of the machine learning model, **b** Network structure generated via Matlab

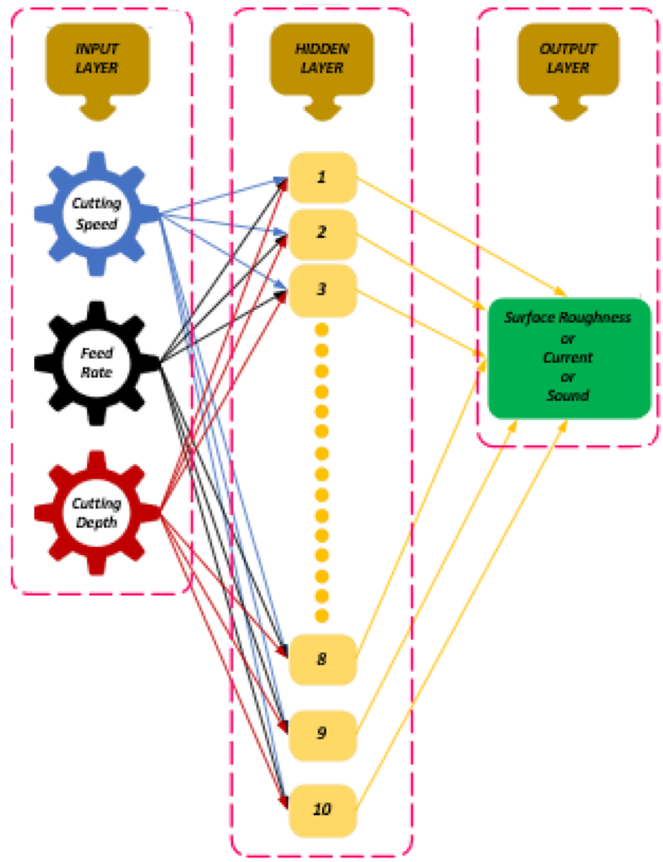

(a)

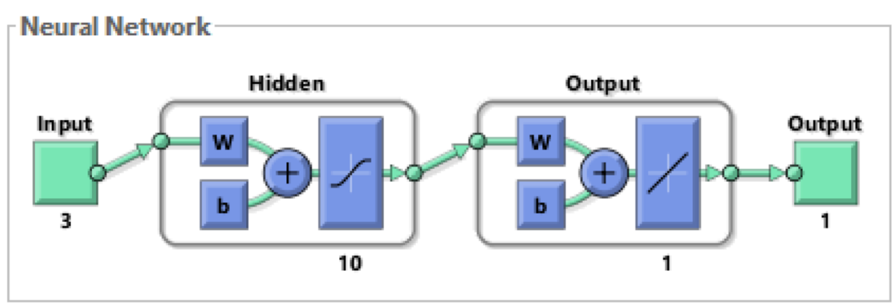

(b)

solution. Abrasion tests were data with Bruker UMT-2-SYS model mechanical test device. Abrasion tests were carried out in the form of micro scratches. Rockwell tip is used as abrasive tip. The scratch length was chosen as 2 mm for all samples. Scratch test was carried out to determine the behavior of hardened AISI 4140 steel material against abrasion. The flowchart of the characterization processes has been Fig. 3.

2.2 Machine Learning Construction and Performance Assessment

The Artificial Neural Network (ANN) represents a machine learning paradigm employed for diverse applications, including classification, data management, regression, and occasionally decision-making. The experimental dataset underwent a tripartite division for training. testing. and verification purposes. The focus of the current study's ANN lies in the estimation and prediction of current, sound, and surface roughness values. The architecture of the ANN in this

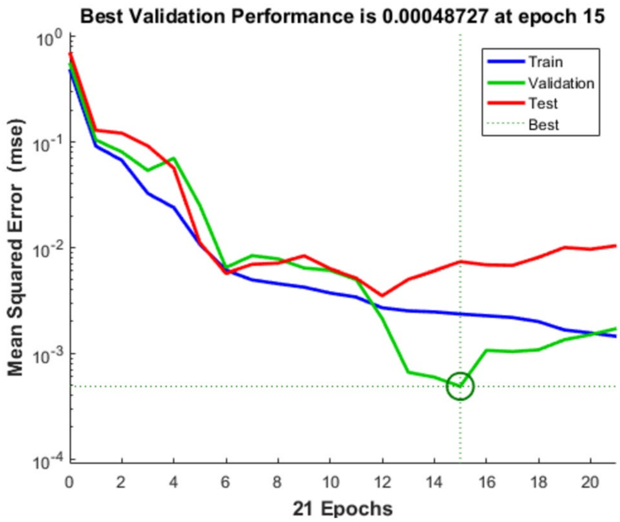

Fig. 6 Variation of MSE worths according to epochs

investigation encompasses both feedforward and backpropagation mechanisms within a multilayer perceptron network construction (Yaseer et al. 2021; Berber and Gürdal 2023), as illustrated in Fig. 4. Following dataset normalization. 70% of the data was allocated for training the ANN model, while the remaining data was utilized for both verification and testing phases.

The MATLAB software (Higham and Higham 2016) suite was employed for computer-aided implementation. facilitating the optimization of the ANN architecture. The configuration of ANN models was executed through the utilization of the 'nftool' command from the command window. Evaluation of Mean Squared Error (MSE) performance and regression analysis for the selected data, which were employed to create and train the network, was conducted using the Neural Fitting module. A schematic representation of the fundamental design of the ANN topology is depicted in Fig. 5.

In the construction of the ANN, a dataset comprising 162 entries derived from experimental findings was employed. To assess the influence of input variables on predictive efficacy, alternative ANN models with varying input variables were generated. The determination of the optimal number of neurons in the hidden layer poses a challenge in the development of ANN structures, as there is no definitive value for this parameter (Saad et al. 2022). However, in this study, a trial-and-error approach was employed, resulting in the identification of the most effective hidden layer structure, which consisted of 10 neurons. Regarding the training algorithm, a comprehensive review of the literature was conducted to identify the most suitable alternatives (Bertolini et al. 2021; Kaveh and Mesgari 2023). The Scaled Conjugate Gradient algorithm, recognized for its superior performance in multilayer perceptron networks, was selected for implementation

Fig. 7 Error histogram of the machine learning construction

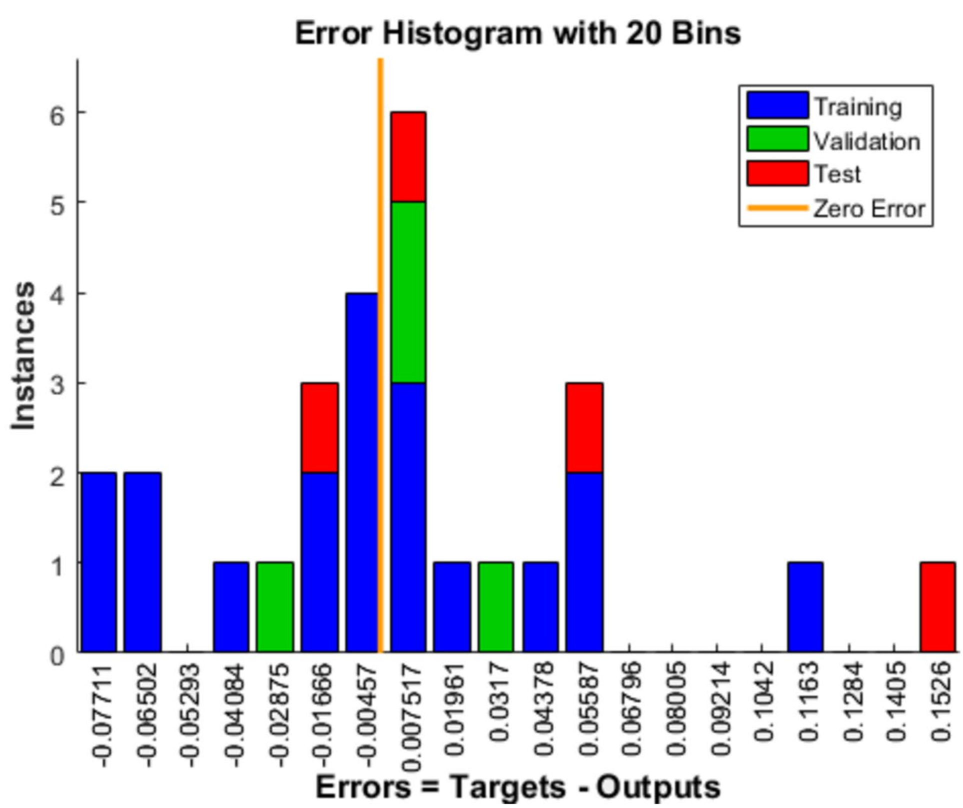

Table 2 Performance comparisons of the hidden layer

Algorithm	Transfer function	Number of neurons	Weight to layer	Bias to layer
Scaled conjugate gradient	Learngdm and Tansig	1	− 0.191	2.888
		2	− 0.310	− 2.765
		3	− 0.407	− 1.424
		4	− 0.380	− 1.023
		5	− 1.216	1.794
		6	− 0.329	0.302
	Best Performance	**7**	**0.0767**	− **0.951**
		8	0.957	3.244
		9	− 0.606	− 3.255
		10	− 0.392	3.205

(Lin et al. 2020; Eser et al. 2021; Yanis et al. 2023a, b). Learngdm and Tansig transfer functions were applied in the hidden and output layers of the perceptron network. The efficiency analysis of the ANN models was conducted in three phases. In the initial phase, the training of the ANN model was executed. The validation of the training phase involved the computation of Mean Squared Error (MSE) variables and a meticulous examination of error histograms. Following the validation of the training phase, the subsequent phase involved scrutinizing the conformity of the estimated values derived from the ANN model with the target values. The final phase comprised an investigation into the performance variables designated for the assessment of performance analysis. To assess the predictive performance of the ANN structure. key metrics such as the correlation coefficient (R^2) and average relative deviation (ARD%) values were scrutinized. Additionally, Fig. 6 presents the Mean Squared Error (MSE) as a determinant for optimal validation performance in the pursuit of an optimal network structure. The adoption of the Scaled Conjugate Gradient (SCG) with a 3–10–1 construction of the ANN yielded lower MSE values. as depicted in Fig. 6. Variations in MSE values during the training process of the optimal network with 10 neurons are illustrated in Fig. 6, highlighting an optimal validation performance of 0.0004827 at epoch 15 (refer to Fig. 7). The evaluation of the ANN structure's performance for testing involved an exploration of different neuron numbers in the hidden layer. with the results presented in Table 2. Notably, the minimum MSE was achieved with 10 neurons in the hidden layer. For instance, weight to layer and bias to layer for the test data in the ideal architecture with 7 neurons were 0.0767 and −0.951, respectively. Experimental data were employed to train the ANN network, and scatter plots depicting the training, validation, testing, and optimal model are illustrated in Fig. 8. In Fig. 8, the horizontal axis represents the target, while the vertical axis signifies the model outputs. An acceptable agreement is indicated when the gradient of the designated line approaches 1 and the perpendicular intersection approaches 0. Three variables, namely the R-value, slope, and y-intercept, were considered in the examination of these graphs. Fundamental balances for output parameters and ANN performance variables used in this study has been demonstrated Table 3.

3 Results and Discussion

3.1 Comparison of Experimental Findings

Since a very good surface quality is required in hard turning, low vibration machine tools should be preferred. The hardness of the material in hard turning increases the force required to remove material from the workpiece. Therefore, the loading intensity on the machine tool increases. Vibration increases when the loading intensity increases on the machine tool. These vibrations cause an increase in the surface roughness value. Therefore, as little as possible depth of cut and feed rate are preferred. In order to obtain a good surface quality in hard turning operations, the machine tool must be rigid.

Figure 9 shows SEM images taken from AISI 4140 surface. When Fig. 9 is examined, cementite grains scattered in martensite blocks are observed. Steels having martensite structure with quenching process, decrease in hardness and increase in toughness by tempering process. (Jagadeeshanayaka et al. 2023). Microstructures consist of acicular martensite and plate martensite. SEM–EDS analysis of AISI 4140 material is given in Fig. 10. Pre-existing martensite affected the growth of bainite hoops and the rate of volume fraction increase. It rapidly evolved to a peak rate due to the acceleration effect of pre-existing martensite with lower volume. Various martensitic transformations are important for steels in terms of hardness. While the room temperature martensite ratio decreased

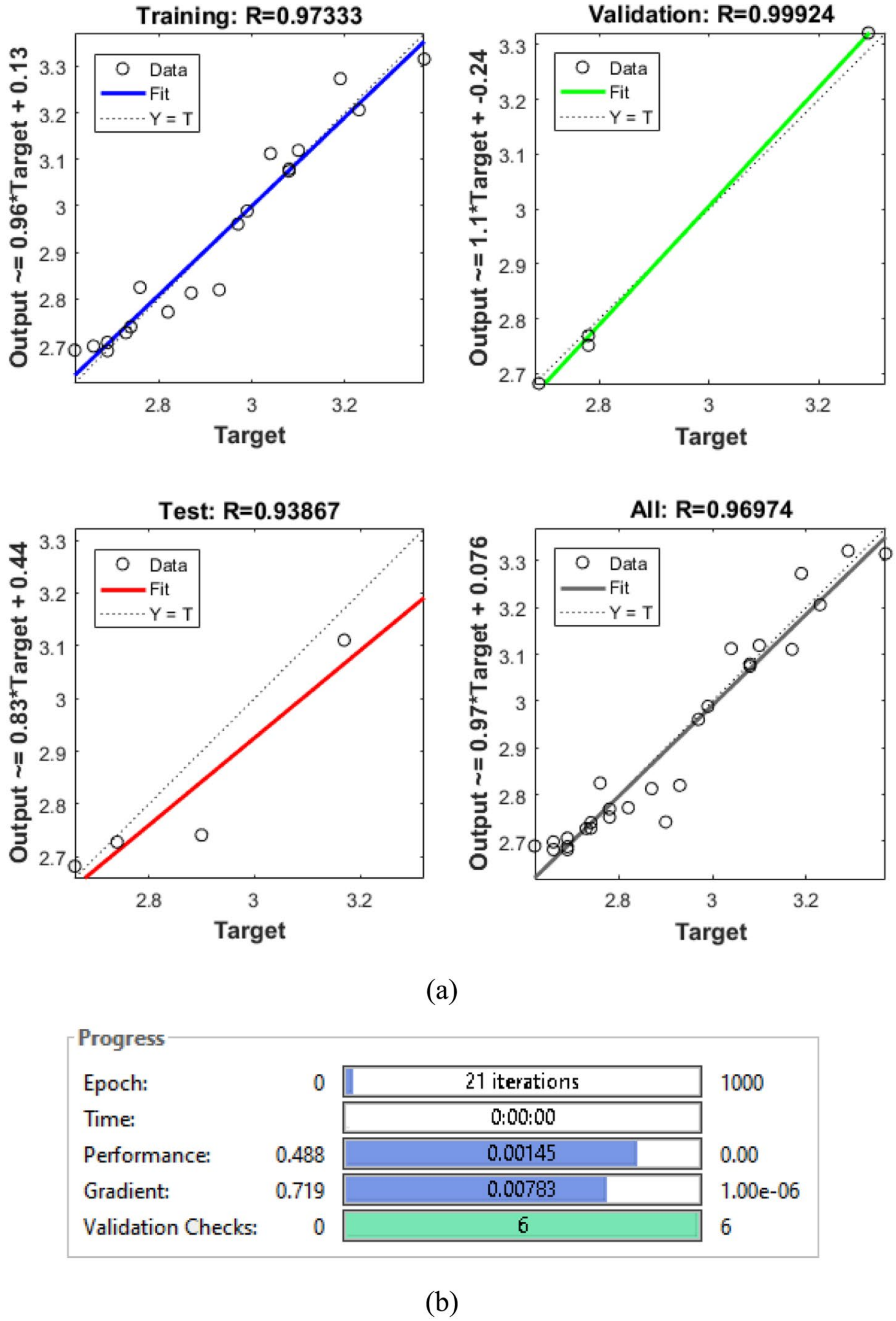

Fig. 8 **a** Regression curves of the neural network construction, **b** time-dependent progress datas

with a slower cooling rate, the auto-tempered martensite ratio increased. A heterogeneous distribution of martensite tetragonality is seen for all cooling rates. It confirms that phase transitions are important in reducing dimensional change by undergoing extra plastic deformation during phase transformations and in strengthening the hard martensitic phase by changing it (Roussos et al. 2023).

When the analysis results given in Fig. 10 are examined, the Fe, Mn, Cr, C, and Mo peaks present in AISI 4140 steel material are clearly seen. The microhardness profiles of the AISI 4140 are given in the Fig. 11. When the analysis results given in Fig. 11 are examined, it is understood that the hard turned material is AISI 4140 steel.

The hardness measurements were taken from the AISI 4140 steel. The hardness of the AISI 4140 material was measured as about 670 $HV_{0.3}$. While making the microhardness measurements of the sample, three different hardness values were obtained and the hardness value was determined

Table 3 Basic data reductions for substantial performance and target variables

Parameter	References	Eq. number	Equation
Surface roughness (µm)	Skrzyniarz et al. (2021)	(1)	$Ra = \left(\frac{P+Q}{L}\right)\frac{1000}{V_q}$
Current (A)	Mahapatra et al. (2022)	(2)	$I = \frac{V}{R}$
Sound (dB)	Muhammad et al. (2023)	(3)	$L = 10\log\left(\frac{w}{w_{ref}}\right)$
Corrosion rate	Srinivasan et al. (1957)	(4)	$I_{corr} = \frac{\beta_a x \beta_c}{2.303 x R_p x(\beta_a+\beta_c)}$
Mean average error	Gurlek et al. (2021)	(5)	$MAE = \frac{1}{n}\sum\left(X_{measured} - X_{estimated}\right)$
Mean square error	Berber and Gürdal (2023)	(6)	$MSE = \frac{1}{n}\sum_{1-i}^{n}\left(X_{measured} - X_{estimated}\right)^2$
Average relative deviation	Gürdal (2023)	(7)	$ARD(\%) = \frac{1}{n}\sum_{1-i}^{n}\left(\left\|\frac{X_{measured}-X_{estimated}}{X_{measured}}\right\|\right)\times 100$
Relation coefficient	Berber et al. (2020)	(8)	$R^2 = 1 - \frac{\sum_{1-i}^{n}\left(X_{measured}-X_{estimated}\right)^2}{\sum_{i-1}^{n}\left(X_{measured}\right)^2}$

by taking the average of these data. The cryogenic process produced a high increase in the hardness of AISI 4140 steel. It increased in hardness in direct proportion with the increase of waiting time of cryogenic process. In the literature, it is emphasized that the cryogenic process has a similar effect on other metallic materials (Kam 2020).

The potentiodynamic polarization curves of the AISI 4140 steel are given in Fig. 12. Corrosion tests of the AISI 4140 steel were performed in 96.5% distilled water and 3.5% NaCl solution. The current was applied between initial E −0.5 mV and final E 0.5 mV against the open cycle potentials determined after 30 min of soaking.

The results of the corrosion measurements are summarized in Table 4. Therefore, corrosion current (Icorr) which can be applied along Tafel curves to corrosion data must be calculated. Corrosion resistance (Rp) values determined from Stern and Geary equation (Srinivasan et al. 1957) can

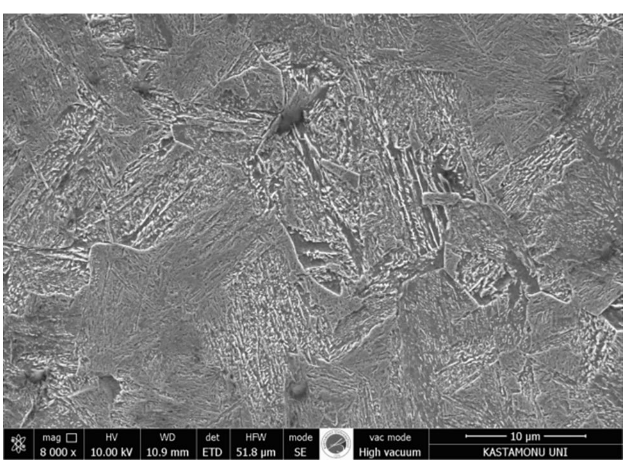

Fig. 9 SEM images of the AISI 4140 steel

also be used to calculate corrosion rates of the AISI 4140 steel in accordance with undermentioned with Eq. (4) in Table 3.

When Table 4 is examined, it is seen that the corrosion resistance of AISI 4140 material has −473 mV. In addition, Rp (corrosion resistance) was calculated as 4.851 kΩ cm^2. From the data obtained. It is clearly seen that the corrosion resistance of AISI 4140 material increases. Similar results are found in the literature for AISI 4140 material (Zohuri 2021). The scratch test graph of the samples can be seen in Fig. 13.

When the graphic is examined, it is understood that the friction coefficient of the AISI 4140 material is ~ 0.08. This is due to the microstructure of double and triple hard phases. These hard phases formed in the AISI 4140 microstructure gave the material strength with dispersion resistance. As a result of all these evaluations, it can be clearly stated that AISI 4140 material is resistant to abrasion. Current value, sound level and surface roughness values obtained as a result of machinability tests on 53 HRC hardness AISI 4140 material are given in Table 5.

3.1.1 Varying of Current Value

The measurement of the current is quite easy. However, it is directly linked to machinability parameters. As the tool wear increases, the instantaneous current value increases. The current value increases when the loads on the machine table increase. As the hardness of the material increases, the tensile strength of the workpiece material increases (Fedai 2023; Yu Pimenov et al. 2023). The current value increases as the tensile strength increases. The relationship between cutting parameters and current values are given in Fig. 14 and Fig. 15.

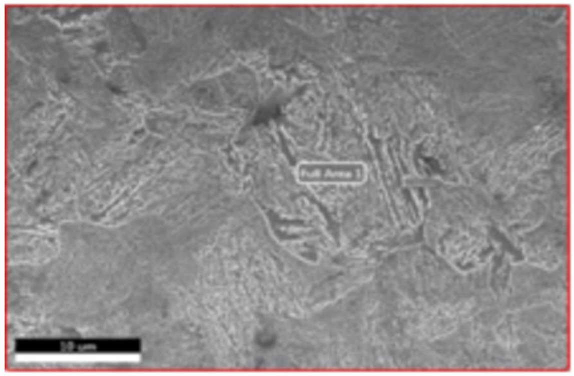

Full Area EDS	
Element	Weight(%)
Fe	79.89
Mn	6.72
Cr	6.61
C	5.38
Mo	1.40

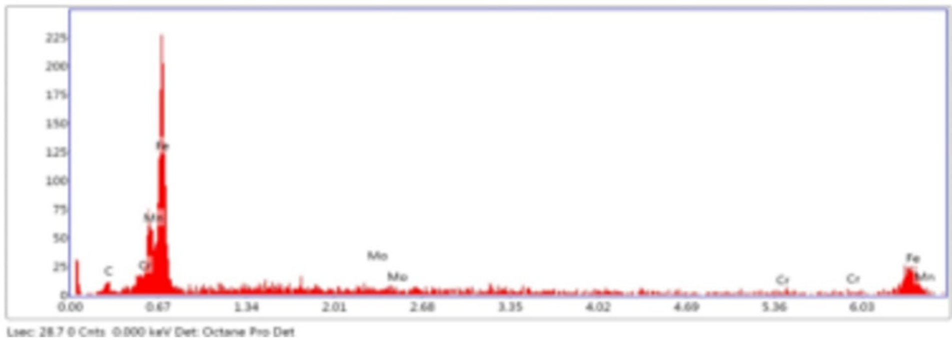

Fig. 10 SEM–EDS analysis of the AISI 4140 steel

The instantaneous current value is also an expression of power consumption. The power consumption increases as the current value increases. Increasing the power consumption or increasing the instantaneous current value indicates that the cutting forces also increase. As the cutting parameters change, the instantaneous current value also changes (Shi et al. 2019; Sousa et al. 2020; Agrawal et al. 2021). When Fig. 14 and Fig. 15 are examined, it is clearly seen that the current value increases with increasing cutting speed. The instantaneous current value increases with the increase in feed rate and depth of cut.

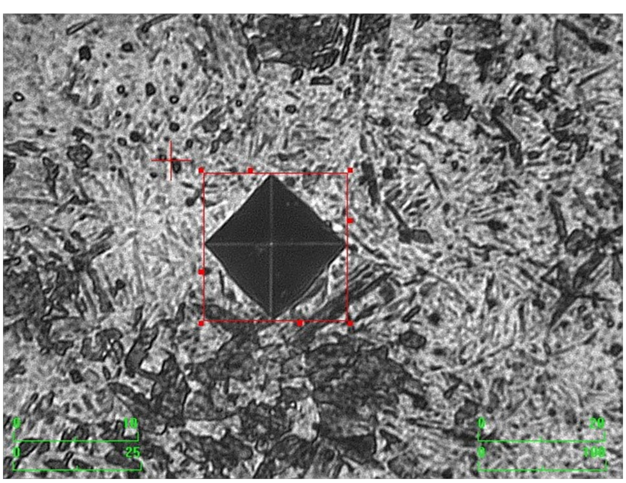

Fig. 11 Hardness indentations of the AISI 4140 steel

3.1.2 Varying of Sound Value

Sound level is an important indicator in controlling the cutting process in the industry. The increase in the sound level and the increase in the instantaneous current value show a similar trend. Because the increase in instantaneous current value is the clearest indicator of the load on the machine tool. As the amount of loading increases, the sound level increases. With the increase in cutting speed, the sound level increases. While the cutting speed has the biggest effect on the change in the sound level, it is followed by the feed rate. Finally, the increase in the depth of cut causes a slight increase in the sound level (Yu Pimenov et al. 2022; Kminiak et al. 2023; Liu et al. 2023). The relationship between the feed rate, cutting speed and sound level are given in Fig. 16 and Fig. 17.

The sound level is an indication of the cutting parameters, vibration, and loading quantities on the machine tool in the manufacturing environment (Fig. 16 and Fig. 17) (Asif et al. 2023). However, in terms of worker health, the sound level should not exceed 93 dB. Therefore, materials were processed within acceptable limits, such as 76 dB.

3.1.3 Varying of Surface Roughness Value

One of the most important parameters in terms of machinability is the surface roughness value. Because the surface roughness value is directly related to friction and friction in machine parts is undesirable. If the roughness value

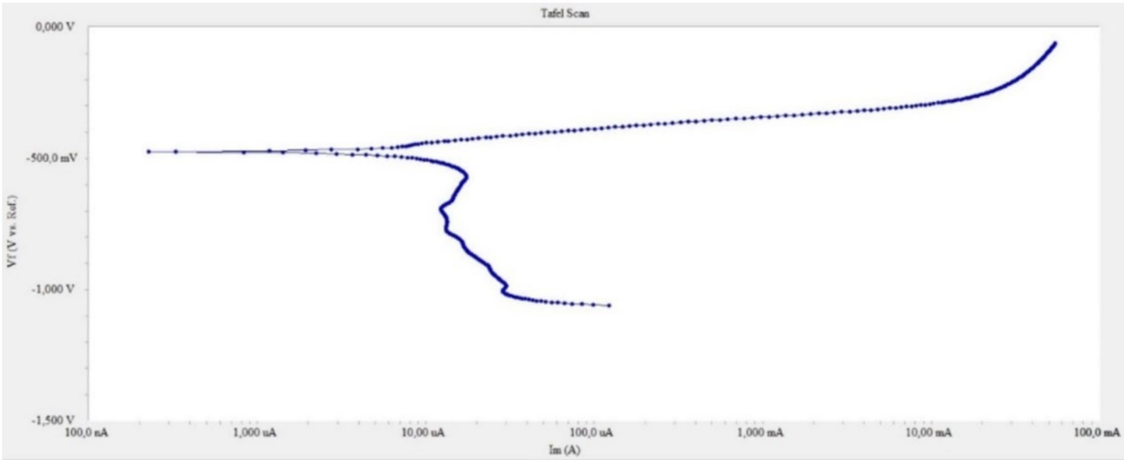

Fig. 12 Potentiodynamic polarization curves of the AISI 4140 steel

Table 4 Electrochemical behaviours of the AISI 4140 steel with a cryogenic process

Material	E_{corr} (mV)	I_{corr} (μAcm^{-2})	B_a (mV)	B_c (mV)	Corrosion rate (mpy)	Corrosion resistance (kΩ cm^2)
AISI 4140	−473	3.600	55.7	144.8	1.732	4.851

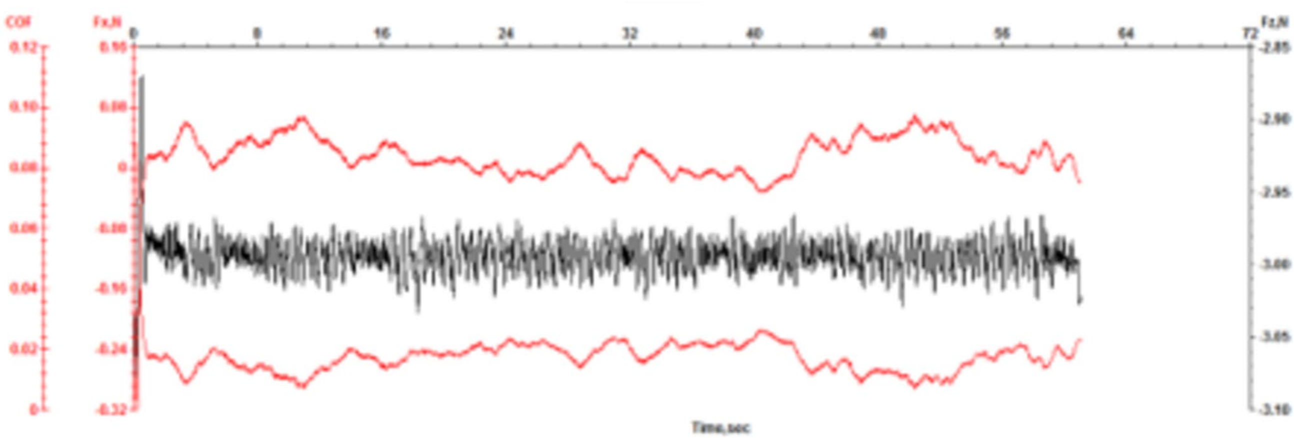

Fig. 13 Scratch test graphic of AISI 4140 material

increases, the friction increases. If the roughness value increases, the wear increases. When the wear increases, the life of the machines is shortened. Energy consumption increases (Reza Kashyzadeh and Ghorbani 2023; Soori and Arezoo 2023). The relationship between cutting parameters and surface roughness value are given in Fig. 18 and Fig. 19.

The most important factor affecting the surface roughness value is the feed rate. If the feed rate increases, the surface roughness value increases. The depth of cut and cutting speed do not have as much influence as the feed rate (Alam et al. 2023; Bag et al. 2023). The surface roughness value up to 1 µm is considered grinding quality. Since these values can be obtained in hard turning, this technique provides a great advantage (Fig. 20).

3.2 ANN Findings of Machinability Characteristics

In this section, the measured and predicted values of the main output parameters roughness, noise and current are compared with reference to the number of experiments. Thus, the prediction performance suitability of the feed forward back propagation neural network can be monitored. The comparison plots for surface roughness, current and sound values are presented in Fig. 21(a), Fig. 21(b) and

Table 5 Machinability test results

Test no	Input parameters			Target parameters		
	a (mm)	V (m/min)	f (mm/rev)	Current (Amper)	Sound L (dB)	Surface Roughness(μm)
1	0.1	160	0.04	2.62	73.1	0.23
2	0.1	160	0.08	2.69	73.4	0.54
3	0.1	160	0.12	2.74	73.5	0.97
4	0.1	200	0.04	2.76	74.1	0.33
5	0.1	200	0.08	2.82	74.4	0.60
6	0.1	200	0.12	2.90	74.6	0.99
7	0.1	240	0.04	2.99	74.7	0.19
8	0.1	240	0.08	3.08	75.5	0.47
9	0.1	240	0.12	3.17	75.9	1.01
10	0.15	160	0.04	2.66	73.4	0.24
11	0.15	160	0.08	2.69	73.6	0.67
12	0.15	160	0.12	2.74	73.8	1.15
13	0.15	200	0.04	2.78	74.1	0.36
14	0.15	200	0.08	2.87	73.9	0.46
15	0.15	200	0.12	2.97	74.3	1.14
16	0.15	240	0.04	3.08	75.6	0.31
17	0.15	240	0.08	3.19	75.7	0.57
18	0.15	240	0.12	3.29	76	1.01
19	0.2	160	0.04	2.66	73.5	0.38
20	0.2	160	0.08	2.69	73.6	0.60
21	0.2	160	0.12	2.73	74	1.02
22	0.2	200	0.04	2.78	74.2	0.43
23	0.2	200	0.08	2.93	74.3	0.57
24	0.2	200	0.12	3.04	74.4	0.93
25	0.2	240	0.04	3.10	75.2	0.37
26	0.2	240	0.08	3.23	75.5	0.59
27	0.2	240	0.12	3.37	75.8	1.00

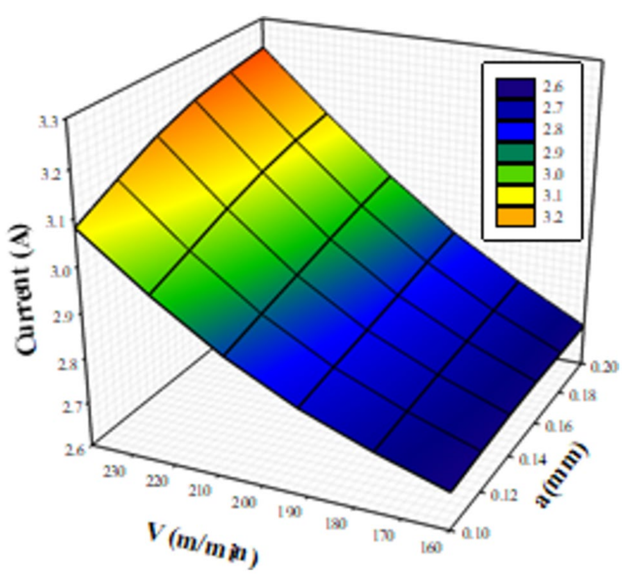

Fig. 14 Varying of current values according to feed rate and cutting speed

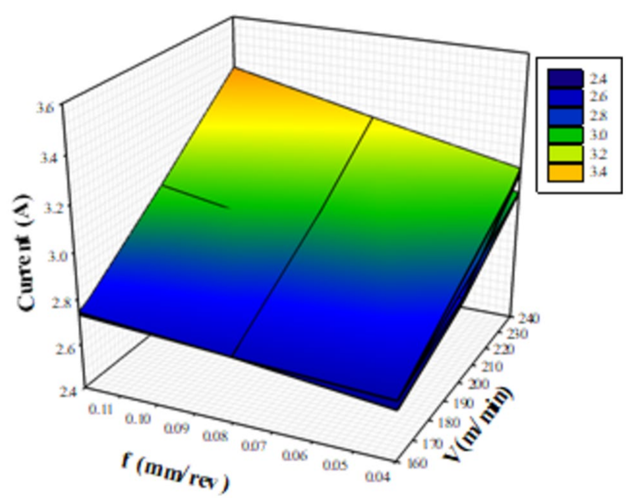

Fig. 15 Varying of current values according to feed rate and cutting depth

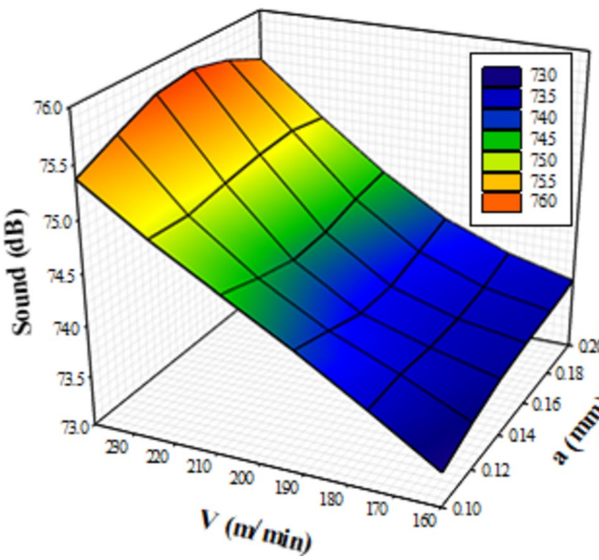

Fig. 16 Varying of sound values according to feed rate and cutting speed

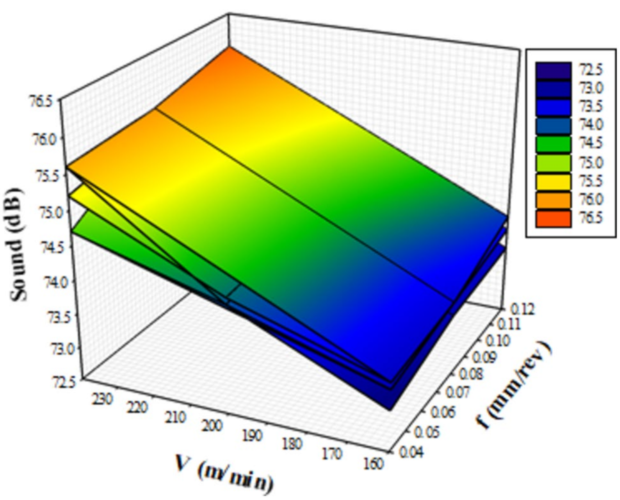

Fig. 17 Varying of sound values according to feed rate and cutting depth

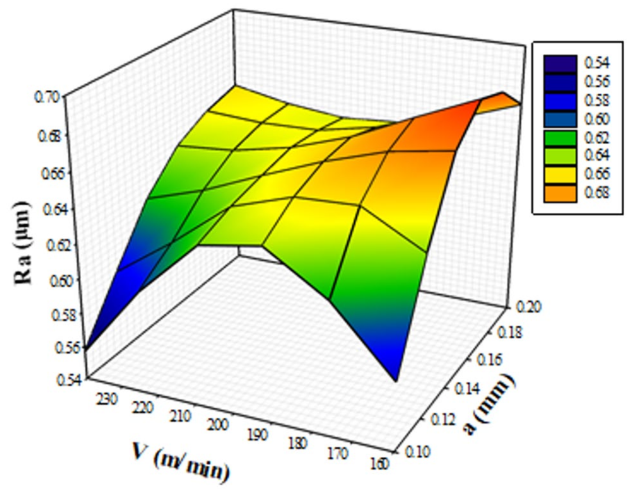

Fig. 18 Varying of roughness values according to feed rate and cutting speed

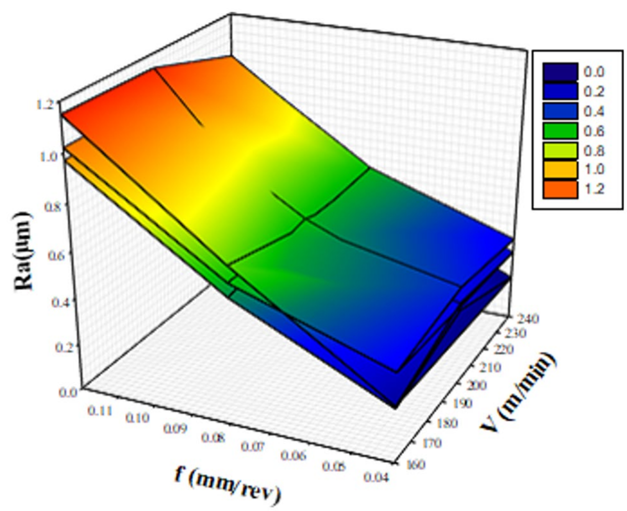

Fig. 19 Varying of roughness values according to feed rate and cutting depth

Fig. 21(c) respectively. Firstly, when the surface roughness comparison graph was examined, it was determined that the measured and predicted finding curves showed similar slopes. The average of the measured and predicted results over the number of experiments are 0.59740 μm and 0.57563 μm respectively. Firstly, when the surface roughness comparison graph was examined, it was determined that the measured and predicted finding curves showed similar slopes. The average of the measured and predicted results over the number of experiments are 0.59740 μm and 0.57563 μm respectively. Similarly, the minimum surface roughness is 0.01000 μm and 0.17837 μm while the maximum is 1.15000 μm and 1.15967 μm respectively. Secondary, when it was investigated in Fig. 21 (b), while the current values show a logarithmic plus slope in each of the 10 experiments, a significant decrease was determined in the next experiment. While the lowest current values were obtained in the first experiment, the highest current was obtained in the 27th experiment. Considering all experiments, the average deviation between the measured and predicted current values is 0.20% while the maximum deviation is 5.47%. The prediction performance of the sound values is compared with the measured values in Fig. 21(c). As in Fig. 21(b), the curve slopes show an increase in the first 10 values and then a sudden decrease. In the following ten experiments,

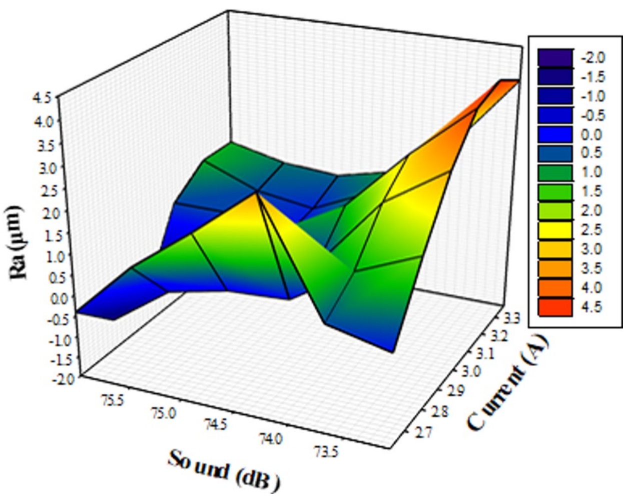

Fig. 20 Comparison of roughness, sound, and current values

a rising and falling trend is observed again. The deviation between the measured and predicted values over a total of 27 experiments is 0.0717% on average. This result clearly shows that the neural network model and optimization is quite appropriate.

The most important parameters and equations that reveal the ANN prediction performance are given in Table 2. The performance comparison of surface roughness, flow and sound prediction results according to the optimized network structure is shown in Fig. 22. The comparison of MAE, MSE, ARD % and R^2 values for these three main output parameters are given in Fig. 22a–d respectively according to the number of experimental data. MAE value specify difference between experimental and forecast output parameters. When this deviation range is lower, the best prediction performance is obtained. In this context, graphic of changing the MAE is examined in Fig. 22(a), it was seen averagely 0.0064, 0.0542, and 0.0218 for current, sound, and surface roughness, respectively. On the other hand, the MSE explains regression's curve state according to the total data. The best forecast are achieved with lower values of MSE (Colak et al. 2022; Bouali et al. 2022). Varying of the MSE with data number has been displayed for all cases in Fig. 22(b). ARD is another important ANN performance parameter. Many studies in the literature show that deviation rates below 10% are acceptable. The predictive bias performances of the three output parameters are presented in Fig. 22(c). When this graph is analyzed, the average ARD% values for current, sound and surface roughness are 0.20%, 0.071%, and 10.71% respectively. These results show that the lowest deviation rates were obtained for sound. Since the roughness values are very small, the smallest deviations increase the ARD value significantly. The coefficient of

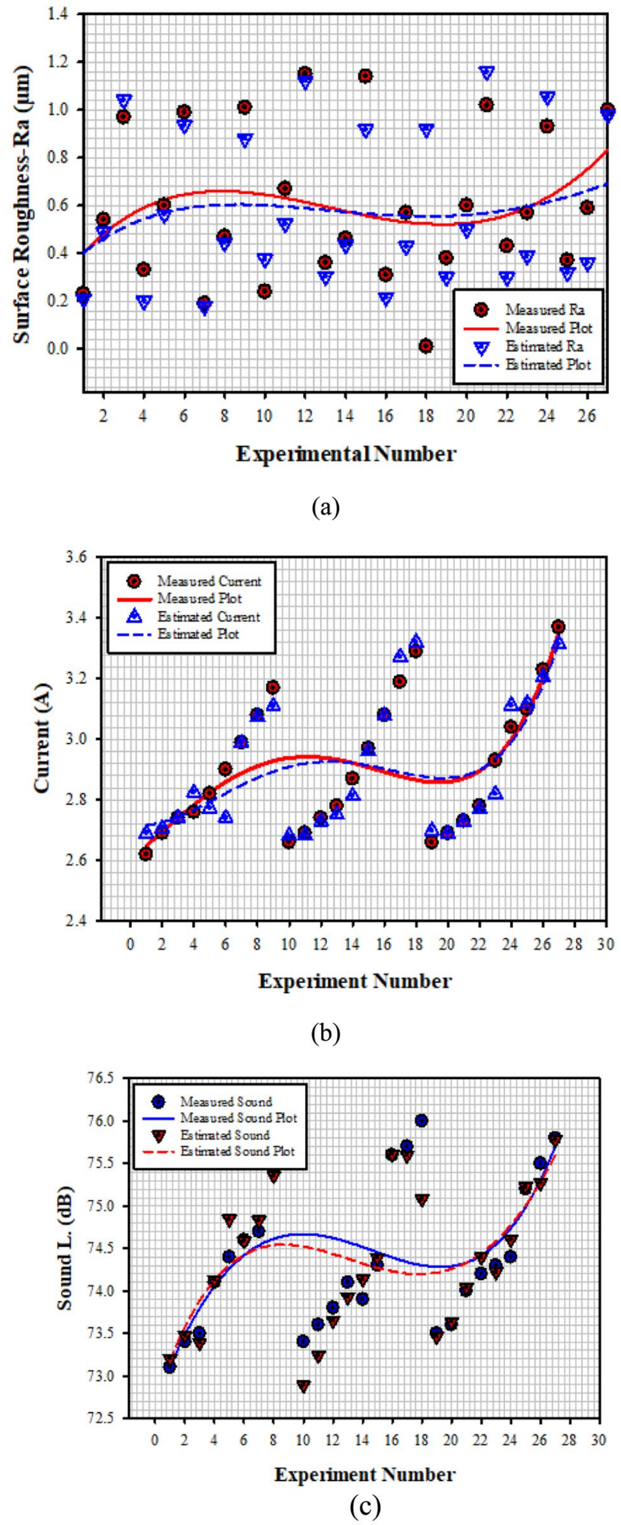

Fig. 21 Comparison of experimental and estimated **a** Ra, **b** sound, **c** current worths

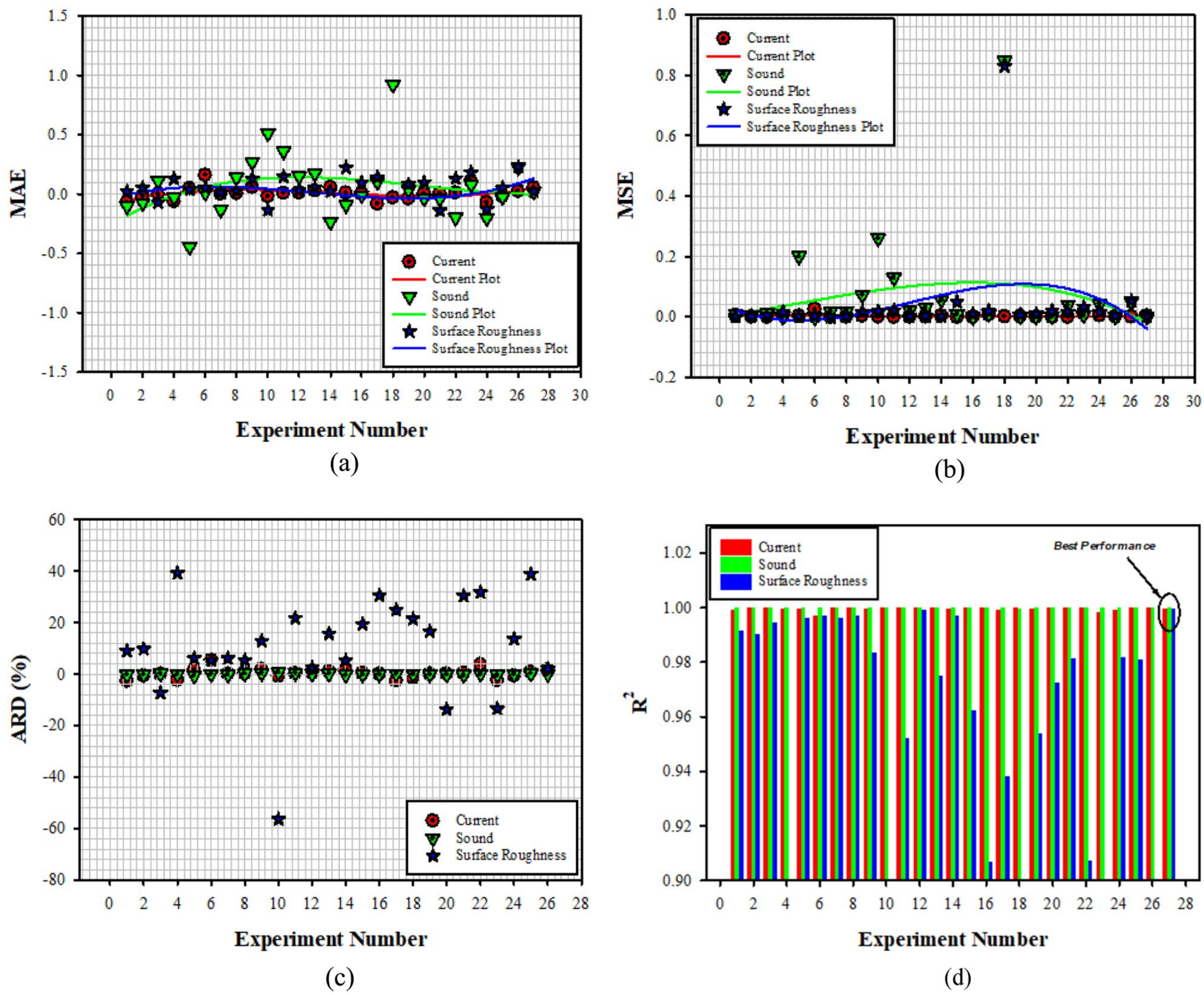

Fig. 22 Comparison of **a** MAE, **b** MSE, **c** ARD, and **d** R^2 performance findings along experimental number

determination, denoted as R^2, serves as an indicator of the extent of linear association existing between the values predicted by a model and those actually observed. This metric is derived by squaring the Pearson correlation coefficient computed for the predicted and observed values. The resultant R^2 values are constrained within the range of 0–1, where a value of 1 signifies an impeccable alignment between predicted and observed values. Notably, a higher R^2 value is indicative of superior model performance. The evaluation methodologies employed in this analysis collectively furnish a thorough evaluation of the precision and dependability of predictions generated by the ANN model. To gain a holistic comprehension of the model's efficacy, it is imperative to consider these metrics collectively, thereby facilitating a comprehensive assessment of its performance. R^2 comparison of the measured and estimated current, sound, and surface roughness are displayed in Fig. 22d. When R^2 worths is investigated this figures for all case, it can be seen that the estimated values are in suitable with the measured findings. The average R^2 values for measured and estimated current, sound, and roughness were achieved as 0.99970, 0.99998, and 0.95120 respectively.

4 Conclusions

This study aims to conduct a comprehensive characterization analysis of cryogenized AISI 4140 steel, assessing its machinability capabilities and introducing a novel dimension by incorporating machine learning techniques for comparison. The primary objective is to scrutinize and contrast the impact of diverse machining parameters on current, sound, and surface roughness through the utilization of an artificial neural network approach. The results obtained in this context are summarized as follows:

Heat treatment increased the material's corrosion resistance by approximately 2 × and abrasion resistance by 3 × over traditional AISI 4140 steel.
With appropriate tools, hard turning achieved a grinding-quality surface. The feed rate significantly influenced surface roughness, where lower rates improved smoothness, while cutting speed and depth had minimal impact.
Cutting speed was the main factor influencing instantaneous current and sound levels, with a 6% increase in sound level at higher speeds. Feed rate and depth of cut had smaller effects. Maximum sound level was 76 dB, which is within machinability standards.
CBN tools proved highly effective in machining 53 HRC hardness material, yielding excellent results for surface roughness, sound levels, and current values.
Neural networks with Learngdm, Tansig, and Scaled Conjugate Gradient (Trainscg) functions showed high predictive accuracy. For neuron 7, optimal prediction metrics included an MAE of 0.0218, MSE of 0.0429, and R^2 values of up to 0.9999, affirming model precision.
This streamlined version captures the essential findings while reducing redundancy and technical details that may not need to be emphasized.

Hard turning experiments can be performed for steel materials of different hardness using wet cutting conditions. On the other hand, new experiments can be performed by changing the values of cutting speed, feed rate and depth of cut, which are hard turning test parameters. Besides, tests that detect mechanical properties such as wear and three-point bending can be added for post-test characterization of the material to be used in the hard turning process. The different artificial neural network algorithms can be also compared and optimized.

Author contributions Mehmet Akkaş: Conceptualization. Methodology. Investigation. Resources. Writing – original draft. Writing – review & editing. Visualization. Mehmet Gürdal: Methodology. Writing – original draft. Conceptualization. Data curation. review & editing.

References

Agrawal A, Goel S, Bin RW, Price M (2015) Prediction of surface roughness during hard turning of AISI 4340 steel (69 HRC). Appl Soft Comput 30:279–286. https://doi.org/10.1016/J.ASOC.2015.01.059
Agrawal C, Wadhwa J, Pitroda A et al (2021) Comprehensive analysis of tool wear, tool life, surface roughness, costing and carbon emissions in turning Ti–6Al–4V titanium alloy: cryogenic versus wet machining. Tribol Int 153:106597. https://doi.org/10.1016/J.TRIBOINT.2020.106597
Agrawal K, Panda A, Sahoo AK (2024) Advancements in tool wear monitoring in turning operations: digital image processing and AI techniques. J Phys: Conf Series, IOP Publishing. 2818(1):012040. https://doi.org/10.1088/1742-6596/2818/1/012040
Akkus H, Asilturk I (2011) Predicting surface roughness of aısı 4140 steel in hard turning process through artificial neural network, fuzzy logic and regression models. Sci Res Essays 6:13. https://doi.org/10.5897/SRE11.120
Alam ST, Tomal ANMA, Nayeem MK (2023) High-speed machining of Ti–6Al–4V: RSM-GA based optimization of surface roughness and MRR. Results Eng 17:100873. https://doi.org/10.1016/J.RINENG.2022.100873
Asakura K, Yan J (2014) Ultraprecision micro grooving on brass for surface wettability control. Adv Mat Res 1017:489–494. https://doi.org/10.4028/WWW.SCIENTIFIC.NET/AMR.1017.489
Asif M, Shen H, Zhou C et al (2023) Recent trends, developments, and emerging technologies towards sustainable ıntelligent machining: a critical review, perspectives future directions. Sustainability 15:8298. https://doi.org/10.3390/SU15108298
ASTM-G102 (2023) Practice for calculation of corrosion rates and related ınformation from electrochemical measurements. https://doi.org/10.1520/G0102-23
Bag R, Panda A, Sahoo AK, Kumar R (2023) Sustainable high-speed hard machining of AISI 4340 steel under dry environment. Arab J Sci Eng 48:3073–3096. https://doi.org/10.1007/S13369-022-07094-9/FIGURES/19
Berber A, Gürdal M (2023) Estimation of forced heat convection in a rectangular channel with curved-winglet vortex generator: a machine learning approach. Therm Sci Eng Prog 37:101563. https://doi.org/10.1016/J.TSEP.2022.101563
Berber A, Gürdal M, Bağırsakçı K (2020) Prediction of heat transfer in a circular tube with aluminum and Cr–Ni alloy pins using artificial neural network. Exp Heat Transf 34:89–95
Bertolini M, Mezzogori D, Neroni M, Zammori F (2021) Machine Learning for industrial applications: A comprehensive literature review. Expert Syst Appl 175:114820. https://doi.org/10.1016/J.ESWA.2021.114820
Bin RW, Goel S, Davim JP, Joshi SN (2016) Parametric design optimization of hard turning of AISI 4340 steel (69 HRC). Int J Adv Manuf Technol 82:451–462. https://doi.org/10.1007/S00170-015-7337-2/METRICS
Bouali A, Mohammedi B, Hanini S (2022) A smart model for the prediction of heat transfer coefficient during flow boiling of nanofluids in horizontal tube. Nano Hybrids Compos 36:89–102. https://doi.org/10.4028/P-9GE01G
Choo SH, Lee S, Golkovski MG (2000) Effects of accelerated electron beam irradiation on surface hardening and fatigue properties in an AISI 4140 steel used for automotive crankshaft. Mater Sci Eng, A 293:56–70. https://doi.org/10.1016/S0921-5093(00)01207-7
Colak AB, Karakoyun Y, Acikgoz O et al (2022) A numerical study aimed at finding optimal artificial neural network model covering experimentally obtained heat transfer characteristics of hydronic underfloor radiant heating systems running various nanofluids. Heat Transf Res 53:51–71. https://doi.org/10.1615/HEATTRANSRES.2022041668
Das SR, Dhupal D, Kumar A (2015a) Experimental investigation into machinability of hardened AISI 4140 steel using TiN coated ceramic tool. Measurement 62:108–126. https://doi.org/10.1016/J.MEASUREMENT.2014.11.008
Das SR, Dhupal D, Kumar A (2015b) Study of surface roughness and flank wear in hard turning of AISI 4140 steel with coated ceramic inserts. J Mech Sci Technol 29:4329–4340. https://doi.org/10.1007/S12206-015-0931-2/METRICS
Eser A, Aşkar Ayyildiz E, Ayyildiz M, Kara F (2021) Artificial ıntelligence-based surface roughness estimation modelling for

milling of AA6061 alloy. Adv Mater Sci Eng. https://doi.org/10.1155/2021/5576600

Fedai Y (2023) Exploring the ımpact of the turning of AISI 4340 steel on tool wear, surface roughness, sound ıntensity, and power consumption under dry, MQL, and nano-MQL conditions. Lubricants 11:442. https://doi.org/10.3390/LUBRICANTS11100442

Gaitonde VN, Karnik SR, Figueira L, Paulo Davim J (2009) Machinability investigations in hard turning of AISI D2 cold work tool steel with conventional and wiper ceramic inserts. Int J Refract Metals Hard Mater 27:754–763. https://doi.org/10.1016/J.IJRMHM.2008.12.007

Gaitonde VN, Karnik SR, Figueira L, Davim JP (2011) Performance comparison of conventional and wiper ceramic inserts in hard turning through artificial neural network modeling. Int J Adv Manuf Technol 52:101–114. https://doi.org/10.1007/S00170-010-2714-3/METRICS

Ginting B, Sembiring RW, Manurung N (2017) Study of surface integrity AISI 4140 as result of hard, dry and high speed machining using CBN. In: Journal of physics: conference series, p 12145

Grzesik W (2008) Influence of tool wear on surface roughness in hard turning using differently shaped ceramic tools. Wear 265:327–335. https://doi.org/10.1016/J.WEAR.2007.11.001

Grzesik W, Żak K, Chudy R (2017) Influence of tool nose radius on the cutting performance and surface finish during hard turning with CBN cutting tools. J Mach Eng 17:56–64

Gürdal M (2023) Artificial intelligence approach for energy and entropy analyses of $NiFe_2O_4/H_2O$ nanofluid flow in a tube with vortex generator. Eng Anal Bound Elem 152:277–292. https://doi.org/10.1016/J.ENGANABOUND.2023.04.016

Gurlek C, Sahin M, Akkoyun S (2021) Estimation of the wind speed in Sivas province by using the artificial neural networks. Wind Struct 32:161–167. https://doi.org/10.12989/WAS.2021.32.2.161

Higham DJ, Higham NJ (2016) MATLAB guide. SIAM, New Delhi

Huang Y, Liang SY (2005) Modeling of cutting forces under hard turning conditions considering tool wear effect. J Manuf Sci Eng 127:262–270. https://doi.org/10.1115/1.1852571

Jadhav PK, Sahai RSN (2024) Sustainable machining of AISI4140 steel: a Taguchi-ANN perspective on ecofriendly metal cutting parameters. J Mater Sci: Mater Eng 19(1):13. https://doi.org/10.1186/s40712-024-00154-y

Jagadeeshanayaka N, Kele SN, Jambagi SC (2023) An investigation into the relative efficacy of high-velocity air-fuel-sprayed hydroxyapatite implants based on the crystallinity index, residual stress, wear, and in-flight powder particle behavior. Langmuir. https://doi.org/10.1021/ACS.LANGMUIR.3C02840

Jamali AR, Khan W, Chandio AD et al (2019) Jamshoro under the CC by 4.0 International License. 755 Mehran Univ Res J Eng Technol 38:2413–7219. https://doi.org/10.3316/INFORMIT.503058662845470

Kam M (2020) Effects of deep cryogenic treatment on machinability, hardness and microstructure in dry turning process of tempered steels. Proc Inst Mech Eng Part E J Process Mech Eng 235:927–936. https://doi.org/10.1177/0954408920979446

Kam M, Saruhan H (2021) Vibration damping capacity of deep cryogenic treated AISI 4140 steel shaft supported by rolling element bearings. Materialpruefung Mater Test 63:742–747. https://doi.org/10.1515/MT-2020-0118/MACHINEREADABLECITATION/RIS

Karayel D (2009) Prediction and control of surface roughness in CNC lathe using artificial neural network. J Mater Process Tech 7:3125–3137. https://doi.org/10.1016/J.JMATPROTEC.2008.07.023

Kaveh M, Mesgari MS (2023) Application of meta-heuristic algorithms for training neural networks and deep learning architectures: a comprehensive review. Neural Process Lett 55:4519–4622. https://doi.org/10.1007/S11063-022-11055-6/TABLES/5

Kminiak R, Němec M, Igaz R, Gejdoš M (2023) Advisability-selected parameters of woodworking with a CNC machine as a tool for adaptive control of the cutting process. Forests 14:173. https://doi.org/10.3390/F14020173

Lin WS, Lee BY, Wu CL (2001) Modeling the surface roughness and cutting force for turning. J Mater Process Technol 108:286–293. https://doi.org/10.1016/S0924-0136(00)00835-9

Lin YC, Da Wu K, Shih WC et al (2020) Prediction of surface roughness based on cutting parameters and machining vibration in end milling using regression method and artificial neural network. Appl Sci 10:3941. https://doi.org/10.3390/APP10113941

Liu Y, Yang W, Deng E et al (2023) Aerodynamic impacts of high-speed trains on city-oriented noise barriers: a moving model experiment. Alex Eng J 68:343–364. https://doi.org/10.1016/J.AEJ.2023.01.041

Mahapatra S, Das A, Jena PC, Das SR (2022) Turning of hardened AISI H13 steel with recently developed S3P-AlTiSiN coated carbide tool using MWCNT mixed nanofluid under minimum quantity lubrication. Proc Inst Mech Eng Part C J Mech Eng Sci 237:843–864. https://doi.org/10.1177/09544062221126357

Mia M, Razi MH, Ahmad I et al (2017) Effect of time-controlled MQL pulsing on surface roughness in hard turning by statistical analysis and artificial neural network. Int J Adv Manuf Technol 91:3211–3223. https://doi.org/10.1007/S00170-016-9978-1/METRICS

Muhammad N, Jamaludin J, Sapit A et al (2023) Aerodynamic analysis on noise from automotive side mirror using CFD. J Emerg Technol Ind Appl 2:1–6

Muthukrishnan N, Davim JP (2009) Optimization of machining parameters of Al/SiC-MMC with ANOVA and ANN analysis. J Mater Process Technol 209:225–232. https://doi.org/10.1016/J.JMATPROTEC.2008.01.041

Neşeli S, Taşdemir Ş, Yaldız S (2009) Prediction of surface roughness on turning with artificial neural network. J Eng Archit Fac Eskiseh Osman Univ 22:65–75

Özel T, Karpat Y (2005) Predictive modeling of surface roughness and tool wear in hard turning using regression and neural networks. Int J Mach Tools Manuf 45:467–479. https://doi.org/10.1016/J.IJMACHTOOLS.2004.09.007

Özel T, Hsu TK, Zeren E (2005) Effects of cutting edge geometry, workpiece hardness, feed rate and cutting speed on surface roughness and forces in finish turning of hardened AISI H13 steel. Int J Adv Manuf Technol 25:262–269. https://doi.org/10.1007/S00170-003-1878-5/METRICS

Özlü B, Akgün M, Demir H (2023) Evaluation of the effect of hot forging and cooling conditions on the microstructure, hardness and machinability of medium carbon DIN 41Cr4 steel. J Fac Eng Archit Gazi Univ 38:231–243. https://doi.org/10.17341/GAZIMMFD.952713

Poulachon G, Moisan A, Jawahir IS (2001) Tool-wear mechanisms in hard turning with polycrystalline cubic boron nitride tools. Wear 250:576–586. https://doi.org/10.1016/S0043-1648(01)00609-3

Rashid WB, Goel S, Luo X (2001) Enabling ultra high precision on hard steels using surface defect machining

Rashid WB (2014) Surface defect machining: a new approach for hard turning. PhD Thesis. Heriot-Watt University

Reza Kashyzadeh K, Ghorbani S (2023) New neural network-based algorithm for predicting fatigue life of aluminum alloys in terms of machining parameters. Eng Fail Anal 146:107128. https://doi.org/10.1016/J.ENGFAILANAL.2023.107128

Risbood KA, Dixit US, Sahasrabudhe AD (2003) Prediction of surface roughness and dimensional deviation by measuring cutting forces and vibrations in turning process. J Mater Process Technol 132:203–214. https://doi.org/10.1016/S0924-0136(02)00920-2

Rooprai RS, Singh H, Singh T, Singla YK (2022) Analysis of the wear properties of through hardened AISI-4140 alloy steel using Taguchi technique. Mater Today Proc 50:661–664. https://doi.org/10.1016/J.MATPR.2021.04.196

Roussos C, Deligiannis S, Ioannidou D, Papapanos G, Tsakiridis PE (2023) Microstructural and mechanicalproperties of laser cladding-Deposited AISI 1060 steel with a mixture of 410L alloy and 4140 alloy Powders. J Mat Eng Perform 1-13. https://doi.org/10.1007/s11665-023-08767-8

Saad MS, Mohd Nor A, Abd Rahim I et al (2022) Optimization of FDM process parameters to minimize surface roughness with integrated artificial neural network model and symbiotic organism search. Neural Comput Appl 34:17423–17439. https://doi.org/10.1007/S00521-022-07370-7/TABLES/11

Sayuti M, Sarhan AAD, Salem F (2014) Novel uses of SiO_2 nanolubrication system in hard turning process of hardened steel AISI4140 for less tool wear, surface roughness and oil consumption. J Clean Prod 67:265–276. https://doi.org/10.1016/J.JCLEPRO.2013.12.052

Sazlı MH (2006) A brief review of feed-forward neural networks. Commun Fac Sci Univ Ank Ser A2 A3 Phys Sci Eng 50:11–17. https://doi.org/10.1501/COMMUA1-2_0000000026

Sharma R (2019) Effect of cutting conditions on surface roughness and cutting forces in hard turning of AISI 4340 steel. Int J Adv Res 5:2

Shi KN, Ren JX, Wang SB et al (2019) An improved cutting power-based model for evaluating total energy consumption in general end milling process. J Clean Prod 231:1330–1341. https://doi.org/10.1016/J.JCLEPRO.2019.05.323

Singh J, Singh Gill S, Dogra M et al (2019) Temperature and cutting force analysis in turning of steel AISI 4140 using advanced ceramics tools. In: IOP conference series: materials science and engineering, vol 495, p 012090. https://doi.org/10.1088/1757-899X/495/1/012090

Skrzyniarz M, Nowakowski L, Miko E, Borkowski K (2021) Influence of relative displacement on surface roughness in longitudinal turning of X37CrMoV5-1 steel. Materials 14:1317. https://doi.org/10.3390/MA14051317

Soori M, Arezoo B (2023) Minimization of Surface roughness and residual stress in grinding operations of Inconel 718. J Mater Eng Perform 32:8185–8194. https://doi.org/10.1007/s11665-022-07721-4

Sousa VFC, Silva FJG, Fecheira JS et al (2020) Cutting forces assessment in CNC machining processes: a critical review. Sensors 20:4536. https://doi.org/10.3390/S20164536

Srinivasan J, Kelly RG, Koleva DA et al (1957) Electrochemical polarization: I. A theoretical analysis of the shape of polarization curves. J Electrochem Soc 104:56. https://doi.org/10.1149/1.2428496

Swain S, Panigrahi I, Sahoo AK et al (2020) Effect of tool vibration on flank wear and surface roughness during high-speed machining of 1040 steel. J Fail Anal Prev 20:976–994. https://doi.org/10.1007/S11668-020-00905-X/TABLES/16

Thiele JD, Melkote SN (1999) Effect of cutting edge geometry and workpiece hardness on surface generation in the finish hard turning of AISI 52100 steel. J Mater Process Technol 94:216–226. https://doi.org/10.1016/S0924-0136(99)00111-9

Yanis M, Mohruni AS, Saputra MAA, Dwipayana H (2023b) Comparison of conjugate gradient and Levenberg-Marquardt algorithms on artificial neural networks for surface roughness prediction in milling AISI 1045. Toward Adapt Res Technol Dev Future Life 2689:070038. https://doi.org/10.1063/5.0117332/2903694

Yanis M, Budiman AY, Mohruni AS et al (2023a) Levenberg-Marquardt, Bayesian-regularization, and scaled conjugate gradient algorithms for predicting surface roughness accuracy on side milling AISI 1045. In: AIP Conference Proceedings, p 2544. https://doi.org/10.1063/5.0117323/2884992

Yaseer A, Chen H, Zhang B (2021) Predicting layer roughness with weaving path in robotic wire arc additive manufacturing using multilayer perceptron. In: 2021 IEEE 11th annual ınternational conference on CYBER technology in automation, control, and ıntelligent systems, CYBER, pp 61–66. https://doi.org/10.1109/CYBER53097.2021.9588272

Yu Pimenov D, Bustillo A, Wojciechowski S et al (2022) Artificial intelligence systems for tool condition monitoring in machining: analysis and critical review. J Intell Manuf 34(5):2079–2121. https://doi.org/10.1007/S10845-022-01923-2

Yu Pimenov D, Kiran M, Khanna N et al (2023) Review of improvement of machinability and surface integrity in machining on aluminum alloys. Int J Adv Manuf Technol 129(11):4743–4779. https://doi.org/10.1007/S00170-023-12630-4

Zain AM, Haron H, Sharif S (2010) Prediction of surface roughness in the end milling machining using artificial neural network. Expert Syst Appl 37:1755–1768. https://doi.org/10.1016/J.ESWA.2009.07.033

Żak K (2017) Cutting mechanics and surface finish for turning with differently shaped CBN tools. Arch Mech Eng 64:347–357

Zohuri B (2021) Thermal effects of high power laser energy on materials. Therm Effects High Power Laser Energy Mater. https://doi.org/10.1007/978-3-030-63064-5/COVER